Basic Medical Research

Optimal time point for evaluation in a chronic peripheral nerve injury rat model: a preclinical study

Wahyu Widodo[1,2,3], Ismail Hadisoebroto Dilogo[2], Achmad Fauzi Kamal[2], Radiana Dhewayani Antarianto[4,5], Puspita Eka Wuyung[6], Nurjati Chairani Siregar[6], Fitri Octaviana[7], Aria Kekalih[8], Heri Suroto[9], Dina Aprilya[3], Anissa Feby Canintika[2]

pISSN: 0853-1773 • eISSN: 2252-8083
https://doi.org/10.13181/mji.oa.257778
Med J Indones. 2026.

Received: September 06, 2024
Accepted: July 15, 2025
Published online: January 15, 2026

Authors' affiliations:
[1]Doctoral Program in Medical Sciences, Faculty of Medicine, Universitas Indonesia, Jakarta, Indonesia, [2]Department of Orthopaedics and Traumatology, Faculty of Medicine, Universitas Indonesia, Cipto Mangunkusumo Hospital, Jakarta, Indonesia, [3]Department of Orthopaedics and Traumatology, Fatmawati Hospital, Jakarta, Indonesia, [4]Department of Histology, Faculty of Medicine, Universitas Indonesia, Jakarta, Indonesia, [5]Stem Cell and Tissue Engineering Research Cluster, Indonesian Medical Education and Research Institute (IMERI), Faculty of Medicine, Universitas Indonesia, Jakarta, Indonesia, [6]Department of Anatomical Pathology, Faculty of Medicine, Universitas Indonesia, Cipto Mangunkusumo Hospital, Jakarta, Indonesia, [7]Department of Neurology, Faculty of Medicine, Universitas Indonesia, Cipto Mangunkusumo Hospital, Jakarta, Indonesia, [8]Department of Community Medicine, Faculty of Medicine, Universitas Indonesia, Jakarta, Indonesia, [9]Department of Orthopaedics and Traumatology, Faculty of Medicine, Universitas Airlangga, Dr. Soetomo General Hospital, Surabaya, Indonesia

Corresponding author:
Wahyu Widodo
Department of Orthopaedics and Traumatology, Faculty of Medicine, Universitas Indonesia, Cipto Mangunkusumo Hospital, Jalan Pangeran Diponegoro No. 71, Kenari, Senen, Central Jakarta 10430, DK Jakarta, Indonesia
Tel/Fax: +62-21-3155996/ +62-21-3929655
E-mail: wahyuwidodo.orthofkui@gmail.com

ABSTRACT

BACKGROUND Peripheral nerve injury (PNI) can cause severe functional disabilities and progresses dynamically over time. Since evaluations held at different time points will yield different results, finding an optimal model for PNI comparison is needed. This study aimed to create an animal model of chronic denervation that simulates the progress of nerve injury.

METHODS 6 male Sprague-Dawley rats underwent complete sciatic nerve transection in their right hind limbs, with severed nerve ends secured to a nearby muscle to prevent nerve regrowth. The rats were sacrificed at 2, 3, and 4 weeks. The assessment included walking analysis (pre- and post-injury), wet muscle weight measurement, and histological examination.

RESULTS Progressive gastrocnemius muscle degeneration was observed at 3 different time points. Minimal degenerative changes were noted at 2 weeks, while extensive fibrosis (83.25 [12.19]% collagen area) appeared in the 4th week. The 3rd-week samples showed lymphocyte infiltrations, muscular atrophy, and progressive fibrosis, making it the best model for chronic PNI.

CONCLUSIONS A 3-week chronic denervation model is proposed as a long-term PNI for further regenerative research.

KEYWORDS animal model, muscular atrophy, muscular dystrophies, peripheral nerve injuries, sciatic nerve

Brachial plexus injury (BPI) is a severe form of peripheral nerve injury (PNI) that results in significant functional impairment and reduced quality of life.[1] PNI affects approximately 13–23 individuals per 100,000.[2] Surgical interventions such as neurolysis, nerve grafting, and nerve transfer are considered gold-standard treatments when performed within the critical window before muscle regeneration capacity declines. However, despite advances in surgical techniques, outcomes remain variable and unpredictable.[3] Regenerative medicine approaches, including direct cell-based therapies and biological scaffolds, have been explored to enhance nerve regeneration.[4]

To ensure experimental models are adaptable, they must closely mimic BPI or other often-overlooked PNIs in humans. Developing a reliable animal model for chronic PNI remains challenging. Rats are commonly used due to

the similarity of their nerve microstructure and injury response to humans,[5] as well as their ease of handling during the regeneration process.

The sciatic nerve is the most widely used model for inducing PNI, typically via crushing, partial or complete transection, or chemically-induced injury.[6–8] However, there is no standardized protocol, with variations in injury methods, timing, and staining techniques.[9–11] This study aimed to establish a reproducible chronic denervation protocol in rats to support further research on nerve regeneration using mesenchymal stem cells.

METHODS

Experimental design

Six male Sprague-Dawley rats (8–12 weeks old, 200–300 g) were selected, taking into account ethical considerations, cost, feasibility, and the need for preliminary data. The rats were obtained from the IPB University Pharmacology Animal Facility and housed at the Animal Research Facilities of the Indonesian Medical Education and Research Institute, Universitas Indonesia. They were maintained under standardized conditions with *ad libitum* access to food. The animals were divided into three groups based on the duration of denervation (2, 3, or 4 weeks) prior to sacrifice. Walking track analysis was conducted both before and after denervation. After euthanasia, the gastrocnemius muscles from both hind limbs were excised, weighed, and submitted for histopathological examination. All surgeries were performed by a single microsurgery-trained fellowship surgeon (WW) and approved by the Ethics Committee of the Faculty of Medicine, Universitas Indonesia (No: ND-190/UN2. F1.DEPT.33/PPM.00.02/2023), following the Animal Research: Reporting of In Vivo Experiments guidelines.

Peripheral nerve model setup

Rats were weighed and anesthetized via intraperitoneal injection of ketamine (10 mg/kg) and xylazine (15 mg/kg). The right hind limb, including the rump and thigh, was shaved using an electric trimmer. All procedures were performed under sterile conditions. The left hind limb served as a healthy control.

After marking anatomical landmarks (knee, hip, and ischial tuberosity), a 1.5 cm incision was made perpendicular to the thigh muscle (Figure 1). Small tenotomy scissors were used to separate the skin from the superficial fascia and expose the underlying muscle. Blunt dissection using a mosquito clamp created a plane between muscles to locate and isolate the sciatic nerve proximally and distally.[12] Denervation was achieved by complete transsection of the sciatic nerve with a No. 15 surgical blade, 5 mm proximal to its trifurcation.[12] The severed nerve ends were sutured to adjacent muscle tissue with 8-0 polypropylene to prevent regeneration. The skin and subcutaneous tissues were closed with 4-0 Vicryl using a simple interrupted technique.[12] Uniform postoperative wound care was provided. Animals were euthanized at 2 weeks (n = 3), 3 weeks (n = 2), or 4 weeks (n = 2) using a lethal injection (200 mg/kg). Gastrocnemius muscles were harvested from both hind limbs. Visible fat and connective tissue were removed before weighing the wet muscle mass.

Walking track analysis

A blinded laboratory assistant conducted walking track analysis before and at the conclusion of the experiment. Measurements included printed length (PL), toe spread (TS), and intermediate toe spread (ITS) for both hind limbs, used to calculate the Sciatic Functional Index (SFI), where 0 indicates normal function and –100 indicates complete disability.[13] To compare experimental and normal limbs during a gait cycle, we measured the distance to the opposite foot (TOF) and paw stride length (PSL) in millimeters.

Muscle histology analysis

Histological preparation was performed by a laboratory assistant and reviewed by an experienced pathologist. Bilateral gastrocnemius muscles were weighed and compared between healthy and paralyzed limbs. Muscles were fixed in 10% formalin for 24 hours, followed by dehydration in graded ethanol (70–100%) over 5 days within a histology cassette. After two washes with xylene, the muscles were embedded in paraffin blocks. The blocks were sliced into 5 µm-thick sections using a microtome, and five random slides per sample were stained with hematoxylin and eosin and Masson's Trichrome (MT) for analysis.[14] Evaluated parameters included skeletal muscle fiber morphology, collagen area fraction, and lymphocyte infiltration.

Images from five randomly selected fields were captured at 4×, 40×, 100×, and 400× magnifications. For muscle histology analysis, images taken at 400×

magnification were analyzed using ImageJ software (National Institutes of Health, USA) to determine fiber size, shape, and distribution before evaluating every myofiber contained within the images.

A longitudinal section was made from each muscle, extending from the Achilles tendon insertion to the mid-gastrocnemius muscle belly. Key parameters assessed in the denervated gastrocnemius muscle and neuromuscular junction (NMJ) included fiber structure (diameter and continuity), fibrosis, lymphocyte infiltration, and satellite cell proliferation. Histological changes in each section were compared with those in normal muscle tissue, particularly the changes commonly observed in skeletal muscle degeneration. This descriptive analysis aimed to identify the similarities and differences between denervated and contralateral healthy muscles.

Collagen organization and lymphocyte infiltration analysis

For histomorphometric analysis of collagen area, MT-stained slides were observed using a light microscope and imager (Zeiss Axiocam; Zeiss, Germany) at 4× objective lens magnification to obtain an overall microscopic image of the preparation. Quantitative histological analysis using ImageJ software (National Institutes of Health) was performed at 40×, 100×, and 400× magnification to assess collagen organization and lymphocyte infiltration.[15] Images were split into red, green, and blue channels: the red channel represented collagen-rich extracellular matrix, while the green channel identified lymphocyte infiltration and putative satellite cells adjacent to the endomysium.

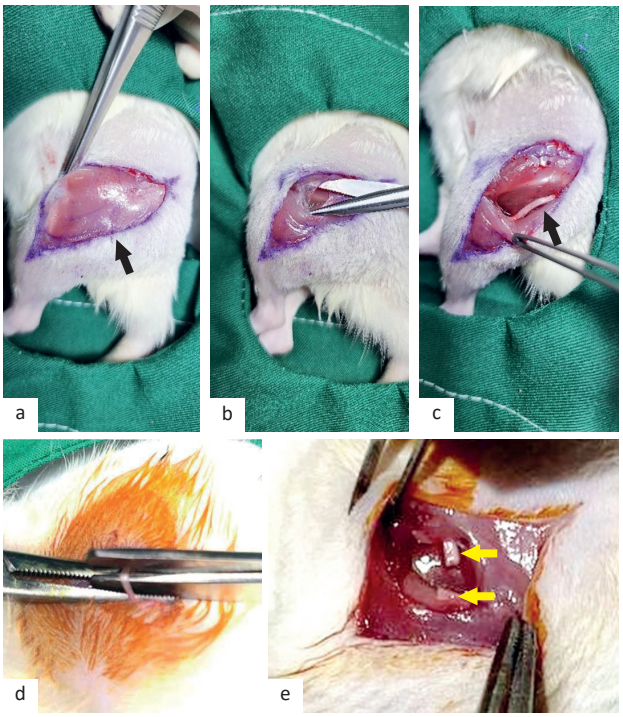

Figure 1. Surgical procedure. (a) Exposure of thigh muscle (black arrow); (b) soft tissue dissection following a loose plane between muscles bundles; (c) sciatic nerve exposure (black arrow); (d) complete nerve transection; (e) both nerve ends were separated and sutured to nearby muscle (yellow arrows)

Statistical analysis

Quantitative histological analysis of the collagen area was performed using ImageJ software (National Institutes of Health). The Shapiro–Wilk test was conducted for normality, and Levene's test for homogeneity. Walking track data were analyzed using the Kruskal–Wallis test. The collagen area fraction and lymphocyte infiltration on the healthy and denervated sides were tested using the Mann–Whitney *U* test. A *p*-value of <0.05 was considered statistically significant. SPSS software version 25.0 (IBM Corp., USA) was used for statistical analyses.

RESULTS

In the present study, we successfully established a chronic PNI model. No mortality or infection was observed in any of the six animals. Gross dissection revealed no spontaneous nerve regeneration. Macroscopic examination showed that the injured limb had reduced muscle mass compared to the non-experimental side, indicating muscle atrophy.

Walking track analysis

All denervated limbs showed a significant increase in TOF and PSL values, along with a decrease in SFI, compared to baseline measurements. Mean (SD) of TOF increased from 30.67 (9.2) to 56.04 (5.64) mm (p = 0.005), and PSL increased from 53.83 (9.53) to 95.31 (14.27) mm (p = 0.003). Although the decline in SFI values was not statistically significant, it decreased from −9.22 (9.17) to −27.05 (42.23) (p = 0.342). Both TOF and PSL tended to increase with longer denervation periods (p = 0.368 and 0.102, respectively) (Figure 2).

Muscle histology analysis

The average weight of the gastrocnemius muscle in the denervated limb was lower (0.75 g) than that in

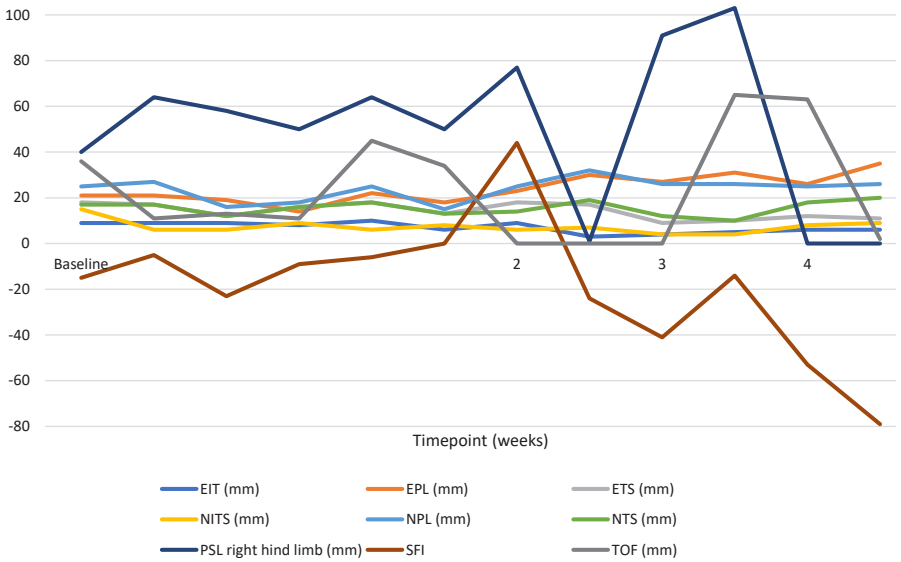

Figure 2. Walking track parameters at the initial measurement and the 2nd, 3rd, and 4th weeks of denervation period. EIT=experimental intermediary toe spread; EPL=experimental print length; ETS=experimental toe stride; NIT=normal intermediary toe spread; NPL=normal print length; NTS=normal toe stride; PSL=paw stride length; SFI=sciatic functional index; TOF=distance to the opposite foot

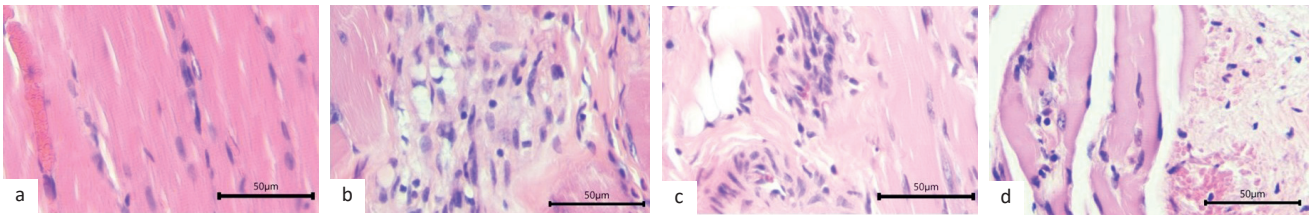

Figure 3. Representative histological microphotographs stained with H&E in HPF taken from rat model in healthy group (a) in comparison to post-sciatic nerve transection after 2 weeks (b), 3 weeks (c), and 4 weeks (d). Observe the progressively increasing infiltration of lymphocyte and fibroblast (blue colors), appearance of fibrotic tissue (pale colors), and disarrangement of muscle fibers (pink colors). H&E=hematoxylin and eosin; HPF=high-power field

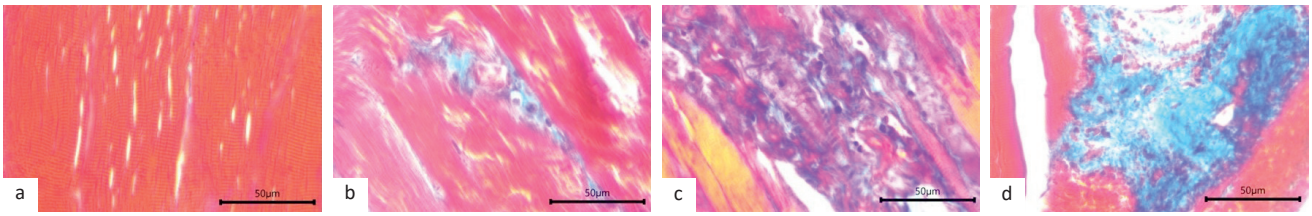

Figure 4. Representative histological microphotographs stained with MT in HPF taken from rat model in healthy group (a), 2 weeks (b), 3 weeks (c), and 4 weeks (d) denervation groups. There is a progressive increase in fibrotic tissue saturation (shown by blue color). HPF=high-power field; MT=Masson's Trichrome

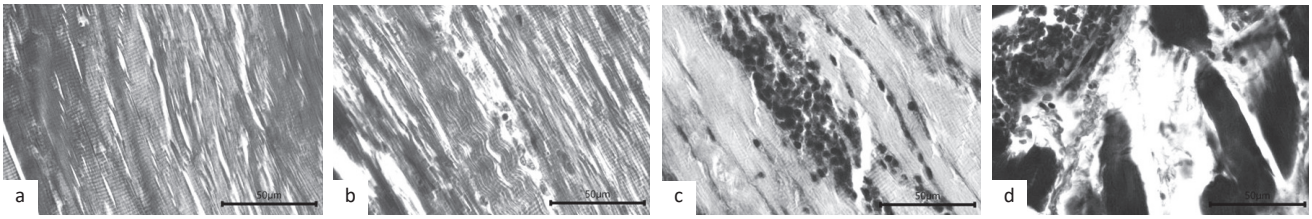

Figure 5. Representative ImageJ processed microphotographs in high-power field (HPF) taken from rat model in: (a) healthy group; (b) 2 weeks terminated post-sciatic nerve complete transection group; (c) 3 weeks terminated post-sciatic nerve complete transection group; (d) 4 weeks terminated post-sciatic nerve complete transection group. Scale bar marked 50 µM. Observe the progressively increasing infiltration of lymphocyte (black) and appearance of fibrotic tissue (white)

the contralateral limb (1.73 g). The 4-week denervation group showed the largest difference in muscle weight between denervated and normal limbs. Histological analysis of the healthy limb demonstrated intact muscle tissue with minimal discontinuity and uniform fiber diameter.

In contrast, histological evaluation of the denervated gastrocnemius muscle revealed notable alterations (Figure 3). Longitudinal sections of the skeletal muscle fibers showed irregular diameters following complete sciatic nerve transection at weeks 2, 3, and 4. Fiber continuity decreased, and striation loss became more prominent with longer denervation durations.

Collagen organization and lymphocyte infiltration analysis

Two weeks after complete sciatic nerve transection, focal lymphocyte infiltration between fibrotic tissues was observed in 20–30% of five random high-power field (HPF) areas. By week 3, up to 70% of these areas of the gastrocnemius muscle showed damage. Chronic PNI progression and associated muscle degeneration continued until week 4, when extensive disorganization of skeletal muscle fibers and widespread fibrotic tissues were observed.

Following chronic PNI, some normal skeletal muscle tissue remained at 2 weeks, although early degenerative changes were evident. By week 3, nearly all skeletal muscle tissue had undergone transformation, characterized by abundant lymphocyte infiltrates, decreasing skeletal muscle fiber size, and replacement by scar tissue in several locations. Satellite cell proliferation was observed, but it was insufficient to compensate for the damaged muscle tissue. At week 4, histological analysis indicated that the satellite cells failed to compensate for muscle damage, leading to the accumulation of a large amount of connective tissue. This excessive connective tissue filled the area between degenerated skeletal muscle fibers, rendering the changes irreversible.

MT staining confirmed progressive fibrotic tissue formation in degenerated skeletal muscle tissue. The collagen area fraction significantly increased following nerve transection. A minimal amount of collagen (0.85 [0.4]%) was present in the fibrotic area of the healthy group. However, in the 4th-week denervation model, the collagen area fraction reached 83.25 (12.19)%, evidenced by blue staining in most HPF areas (Figure 4).

Lymphocyte infiltration counts were analyzed for each group of microphotographs, revealing an increase in lymphocyte infiltration per HPF. No infiltration was observed in the healthy group, whereas in the 4th-week group, lymphocytes were widespread, reaching 39 (range: 13–73) per HPF (Figure 5).

DISCUSSION

This study demonstrates that 3 weeks of PNI may represent a critical threshold between reversible and irreversible muscle degeneration. The "point of no return" in PNI remains poorly defined, contributing to variability in treatment timing. Early reinnervation surgery is essential to prevent irreversible neuromuscular deterioration; however, delayed presentation is common among patients.[16,17] Various studies have explored strategies to improve poor prognosis, such as combining regenerative medicine with conventional surgical techniques or novel approaches. This proposed chronic nerve injury model mimics real-world patient conditions observed in outpatient clinics.

Various physiological conditions, including aging, corticosteroid exposure, immobility, and denervation, have been incorporated into animal models to understand the nature of muscle atrophy. In rats, denervation-induced muscle degeneration begins immediately, and can lead to a 50% reduction in muscle volume within 2 weeks, a process that occurs over 2 months in humans. This volume reduction, accompanied by progressive contractility impairment and muscle atrophy, results in poor outcomes and impaired functional efficacy.[18,19]

Several studies have shown that chronic denervation can lead to progressive changes in muscle tissue. Stonnington and Engel[20] reported up to 80% gastrocnemius atrophy within 1 week of sciatic nerve transection. In contrast, Torrejais et al[21] found minimal changes at 2 weeks, more severe effects in diaphragm muscle of rats after 8 weeks, and progressive damage in gastrocnemius muscle between 2 and 4 weeks of chronic denervation. The walking track analysis showed worsening functional performance over time, with the most pronounced deficits in the 4th week. The PSL and TOF values provided evidence of a disabled right hind limb (denervated limb), causing a delayed step cycle.

Denervation-induced muscle degeneration progresses rapidly and is marked by collagen

deposition (fibrosis), fat and lymphocyte infiltration, and loss of skeletal muscle mass (atrophy), strength, and myofiber size. In humans, these changes occur within 2 months of denervation and reach a plateau at approximately 4 months, leading to a 60–80% loss of muscle volume.[22,23] We assessed muscle atrophy severity through wet muscle weight, fiber morphology changes, fibrosis rate, and lymphocyte infiltration at three different time points. The results showed that denervated limbs were significantly lighter than normal limbs, and the 4th-week model exhibited the largest discrepancy between normal and denervated limbs. This difference may be due to greater atrophy of the denervated limb or increased overall weight as the animals live longer. In the uninjured gastrocnemius muscle, we observed normal morphology characterized by homogeneous polygonal muscle fiber distribution with minimal intra-myofiber gaps, lymphocyte infiltration, and collagen fraction area. This matches the findings of Lee et al,[24] who observed that in a mouse denervated model (contralateral limb), the normal tibialis anterior muscle also showed a regularly polygonal-shaped fiber distribution without any evidence of gapping, cell infiltration, or collagen area, which represents fibrosis.

Paudyal et al[19] studied adult and aged rats and found that a 2-week denervation model did not significantly alter muscle fiber morphology, recommending a 4-week or longer model for more apparent changes. In this study, we observed normal muscle fibers with minimal fibrotic changes at this stage. At this point, nerve reconstruction or repair can be beneficial because many functioning muscle fibers are still activated once the signal arrives at the motor endplate (MEP). In humans, MEP increases within muscles, but functional reinnervation is unlikely after 12 months due to progressive fibrosis.[25] By the 4th week, our model closely resembles this condition with extensive fibrosis (>70%), leaving no room for muscle regeneration. The remaining muscle fibers showed irregularities and discontinuities. Similarly, in another model of 28-day denervated hind limb muscles, sciatic nerve transection led to an irregular arrangement of fibers, an increased inter-myofiber gap, fibrotic changes, and massive lymphocyte infiltration.[24]

Lymphocyte infiltration within the muscle is another indicator of muscle degeneration, as chronic inflammatory cells invade skeletal muscle in the absence of electrical stimulation. In combination with transforming growth factor-beta 1 (TGF-β1), this infiltration facilitates crosstalk between parenchymal, inflammatory, and collagen-producing cells, promoting fibrosis.[26] Morrison et al[27] demonstrated that lymphocyte depletion affects TGF-β1 expression, which in turn influences intramuscular collagen accumulation in the *mdx* mouse model. In our study, both lymphocyte infiltration and collagen area fraction increased over time, peaking in the 4-week denervation model. These findings suggest that the 4-week denervation model is unsuitable for nerve regeneration research, as degenerative changes have become irreversible.

The arrival of axonal sprouts from the proximal stump to the distal nerve segment does not necessarily equate to functional nerve recovery.[23] The regenerative capacity of muscle and the NMJ is key to successful nerve surgery. Skeletal muscle regeneration from atrophy is mediated by a cascade of intrinsic and extrinsic signals that drive myogenesis via satellite cells into functional muscle fibers.[25] Satellite cells possess myogenic, osteogenic, and adipogenic potential and co-express myoblast determination protein 1 (MyoD), a key transcription factor that facilitates differentiation into myocytes within the appropriate niche.[28,29] Suroto et al[30] identified MyoD as a key predictor of muscle regeneration, showing that its expression declined to near zero by 6 months post-injury in humans. This supports the widely accepted 6-month window for brachial plexus or peripheral nerve reconstruction. Although our study did not directly detect satellite cells or their markers, their activity is indirectly supported by the preserved muscle fiber morphology and structure seen in the gastrocnemius muscle up to 3 weeks post-denervation.

According to the gross calculation of the rat-to-human lifespan conversion proposed by Quinn[31] (16.7 rat days = one human year), a 3-week period in rats may be equal to 15 months in humans. However, Suroto et al[30] noted that from a muscle degeneration standpoint, 15 months of denervation in humans typically results in severe and irreversible muscle dystrophy, as regenerative capacity significantly declines after 6 months. Carraro et al[32] also observed similarities in severely atrophic muscle fibers between 7-month denervated rat muscles and 30-month denervated human muscles (post-spinal cord injury), distinguishing these from early myotubes using both morphological features and molecular criteria. Based

on this, 3 weeks of rat denervation may equal 12 weeks in humans, which remains within the golden period for reinnervation. Therefore, we propose the 3-week denervation model for studying chronic nerve injury repair and reconstruction, including nerve transfer and grafting procedures.

This study holds substantial potential for research requiring chronic PNI models, such as stem cell therapy, nerve wrapping, and nerve/target organ preservation. Fibrotic change, in particular, is a valuable endpoint for evaluating antifibrotic agents, fibrinolytics, or preventive therapies, including stem cells with immunomodulatory properties. In conclusion, the 3-week chronic denervation model represents a promising and practical approach to replicating chronic PNI.

This study had some limitations. The study's validity is limited by the small sample size. More frequent assessments (e.g., daily measurement) may yield more precise results. Additionally, only a single sharp nerve injury model was used, which differs from real-world cases that often involve combined nerve and muscle trauma. We also did not evaluate motor function using electromyography (EMG). Future studies would benefit from EMG-based assessments of motor unit action potentials to more accurately characterize chronic PNI.

In conclusion, a 3-week chronic denervation period in rats represents an optimal and clinically relevant model for chronic PNI. At 3 weeks, muscle degeneration is significant but potentially reversible, in contrast to minimal changes at 2 weeks and severe, irreversible fibrosis at 4 weeks. Thus, the 3-week time point offers a critical window for studying interventions aimed at promoting nerve regeneration.

Conflict of Interest

The authors affirm no conflict of interest in this study.

Acknowledgment

None.

Funding Sources

None.

REFERENCES

1. Suroto H, Wardhani IL, Haryadi RD, Aprilya D, Samijo S, Pribadi F. The relationship between patient factors and clinical outcomes of free functional muscle transfer in patients with complete traumatic brachial plexus injury. Orthop Res Rev. 2022;14:225–33.
2. Zhang S, Huang M, Zhi J, Wu S, Wang Y, Pei F. Research hotspots and trends of peripheral nerve injuries based on web of science from 2017 to 2021: a bibliometric analysis. Front Neurol. 2022;13:872261.
3. Suroto H, Rahman A. Traumatic brachial plexus injury: proposal of an evaluation functional prognostic scoring system. Br J Neurosurg. 2021;38(3):643–7.
4. Sumarwoto T, Suroto H, Mahyudin F, Utomo DN, Romaniyanto, Tinduh D, et al. Role of adipose mesenchymal stem cells and secretome in peripheral nerve regeneration. Ann Med Surg (Lond). 2021;67:102482.
5. Tos P, Ronchi G, Papalia I, Sallen V, Legagneux J, Geuna S, et al. Methods and protocols in peripheral nerve regeneration experimental research: part i—experimental models. Int Rev Neurobiol. 2009;87:47–79.
6. Li A, Pereira C, Hill EE, Vukcevich O, Wang A. *In vitro*, *in vivo* and *ex vivo* models for peripheral nerve injury and regeneration. Curr Neuropharmacol. 2022;20(2):344–61.
7. Savastano LE, Laurito SR, Fitt MR, Rasmussen JA, Gonzalez Polo V, Patterson SI. Sciatic nerve injury: a simple and subtle model for investigating many aspects of nervous system damage and recovery. J Neurosci Methods. 2014;227:166–80.
8. Sakuma M, Gorski G, Sheu SH, Lee S, Barrett LB, Singh B, et al. Lack of motor recovery after prolonged denervation of the neuromuscular junction is not due to regenerative failure. Eur J Neurosci. 2016;43(3):451–62.
9. Amniattalab A, Mohammadi R. Functional, histopathological and immunohistichemical assessments of cyclosporine a on sciatic nerve regeneration using allografts: a rat sciatic nerve model. Bull Emerg Trauma. 2017;5(3):152–9.
10. DeLeonibus A, Rezaei M, Fahradyan V, Silver J, Rampazzo A, Bassiri Gharb B. A meta-analysis of functional outcomes in rat sciatic nerve injury models. Microsurgery. 2021;41(3):286–95.
11. Siwei Q, Ma N, Wang W, Chen S, Wu Q, Li Y, et al. Construction and effect evaluation of different sciatic nerve injury models in rats. Transl Neurosci. 2022;13(1):38–51.
12. Bennet GJ, Xie YK. A peripheral mononeuropathy in rat that produces disorders of pain sensation like those seen in man. Pain. 1988;33(1):87–107.
13. de Medinaceli L, Freed WJ, Wyatt RJ. An index of the functional condition of rat sciatic nerve based on measurements made from walking tracks. Exp Neurol. 1982;77(3):634–43.
14. Fischer AH, Jacobson KA, Rose J, Zeller R. Hematoxylin and eosin staining of tissue and cell sections. CSH Protoc. 2008;2008:pdb.prot4986.
15. Dubuisson N, Versele R, Planchon C, Selvais CM, Noel L, Abou-samra M, et al. Histological methods to assess skeletal muscle degeneration and regeneration in duchenne muscular dystrophy. 2022;23(24):16080.
16. Sumarwoto T, Suroto H, Mahyudin F, Utomo DN, Hadinoto SA, Abdulhamid M, et al. Brachial plexus injury: recent diagnosis and management. Open Access Maced J Med Sci. 2021;9(F):13–24.
17. Suroto H, Antoni I, Siyo A, Steendam TC, Prajasari T, Mulyono HB, et al. Traumatic brachial plexus injury in indonesia: an experience from a developing country. J Reconstr Microsurg. 2022;38(7):511–23.
18. Ryu B, Je JG, Jeon YJ, Yang HW. Zebrafish model for studying dexamethasone-induced muscle atrophy and preventive effect of maca (*Lepidium meyenii*). Cells. 2021;10(11):2879.
19. Paudyal A, Slevin M, Maas H, Degens H. Time course of denervation-induced changes in gastrocnemius muscles of adult and old rats. Exp Gerontol. 2018;106:165–72.
20. Stonnington HH, Engel AG. Normal and denervated muscle. A morphometric study of fine structure. Neurology. 1973;23(7):714–24.
21. Torrejais MM, Soares JC, Matheus SM, Francia-Farje LA, Mello JM, Vicente EJ. Morphologic alterations resulting from denervation of the diaphragm in rats. Int J Morphol. 2012;30(3):1150–7.
22. Park HR, Lee GS, Kim IS, Chang JC. Brachial plexus injury in adults. Nerve. 2017;3(1):1–11.
23. Mohammadi R, Vahabzadeh B, Amini K. Sciatic nerve regeneration induced by transplantation of in vitro bone marrow stromal cells into an inside-out artery graft in rat. J

Craniomaxillofacial Surg. 2014;42(7):1389–96.
24. Lee JI, Gurjar AA, Talukder MA, Rodenhouse A, Manto K, O'Brien M, et al. A novel nerve transection and repair method in mice: histomorphometric analysis of nerves, blood vessels, and muscles with functional recovery. Sci Rep. 2020;10(1):21637.
25. Le Grand F, Rudnicki MA. Skeletal muscle satellite cells and adult myogenesis. Curr Opin Cell Biol. 2007;19(6):628–33.
26. Bersini S, Gilardi M, Mora M, Krol S, Arrigoni C, Candrian C, et al. Tackling muscle fibrosis: from molecular mechanisms to next generation engineered models to predict drug delivery. Adv Drug Deliv Rev. 2018;129:64–77.
27. Morrison J, Palmer DB, Cobbold S, Partridge T, Bou-Gharios G. Effects of T-lymphocyte depletion on muscle fibrosis in the *mdx* mouse. Am J Pathol. 2005;166(6):1701–10.
28. Hill M, Wernig A, Goldspink G. Muscle satellite (stem) cell activation during local tissue injury and repair. J Anat. 2003;203(1):89–99.
29. Cooper RN, Tajbakhsh S, Mouly V, Cossu G, Buckingham M, Butler-Browne GS. In vivo satellite cell activation via Myf5 and MyoD in regenerating mouse skeletal muscle. J Cell Sci. 1999;112(Pt 17):2895–901.
30. Suroto H, Wardana GR, Sugianto JA, Aprilya D, Samijo S. Time to surgery and myo-d expression in biceps muscle of adult brachial plexus injury: a preliminary study. BMC Res Notes. 2023;16(1):51.
31. Quinn R. Comparing rat's to human's age: how old is my rat in people years? Nutrition. 2005;21(6):775–7.
32. Carraro U, Boncompagni S, Gobbo V, Rossini K, Zampieri S, Mosole S, et al. Persistent muscle fiber regeneration in long term denervation. past, present, future. Eur J Transl Myol. 2015;25(2):4832.